BET N-terminal bromodomain inhibition selectively blocks Th17 cell differentiation and ameliorates colitis in mice

Kalung Cheung[a,1], Geming Lu[b,c,1], Rajal Sharma[a], Adam Vincek[a], Ruihua Zhang[b,c], Alexander N. Plotnikov[a], Fan Zhang[a,b], Qiang Zhang[a,d], Ying Ju[d], Yuan Hu[b,c], Li Zhao[d], Xinye Han[d], Jamel Meslamani[a], Feihong Xu[b,c], Anbalagan Jaganathan[a], Tong Shen[a], Hongfa Zhu[e], Elena Rusinova[a], Lei Zeng[a,d], Jiachi Zhou[a], Jianjun Yang[b,c], Liang Peng[b,c], Michael Ohlmeyer[a], Martin J. Walsh[a,f], David Y. Zhang[e], Huabao Xiong[b,c,2], and Ming-Ming Zhou[a,2]

[a]Department of Pharmacological Sciences, Icahn School of Medicine at Mount Sinai, New York, NY 10029; [b]Department of Medicine, Icahn School of Medicine at Mount Sinai, New York, NY 10029; [c]Institute of Immunology, Icahn School of Medicine at Mount Sinai, New York, NY 10029; [d]Institute of Epigenetic Medicine, The First Hospital of Jilin University, Changchun 130061, China; [e]Department of Pathology, Icahn School of Medicine at Mount Sinai, New York, NY 10029; and [f]Department of Pediatrics, Icahn School of Medicine at Mount Sinai, New York, NY 10029

Edited by Dinshaw J. Patel, Memorial Sloan Kettering Cancer Center, New York, NY, and approved January 31, 2017 (received for review September 25, 2016)

T-helper 17 (Th17) cells have important functions in adaptor immunity and have also been implicated in inflammatory disorders. The bromodomain and extraterminal domain (BET) family proteins regulate gene transcription during lineage-specific differentiation of naïve CD4$^+$ T cells to produce mature T-helper cells. Inhibition of acetyl-lysine binding of the BET proteins by pan-BET bromodomain (BrD) inhibitors, such as JQ1, broadly affects differentiation of Th17, Th1, and Th2 cells that have distinct immune functions, thus limiting their therapeutic potential. Whether these BET proteins represent viable new epigenetic drug targets for inflammatory disorders has remained an unanswered question. In this study, we report that selective inhibition of the first bromodomain of BET proteins with our newly designed small molecule MS402 inhibits primarily Th17 cell differentiation with a little or almost no effect on Th1 or Th2 and Treg cells. MS402 preferentially renders Brd4 binding to Th17 signature gene loci over those of housekeeping genes and reduces Brd4 recruitment of p-TEFb to phosphorylate and activate RNA polymerase II for transcription elongation. We further show that MS402 prevents and ameliorates T-cell transfer-induced colitis in mice by blocking Th17 cell overdevelopment. Thus, selective pharmacological modulation of individual bromodomains likely represents a strategy for treatment of inflammatory bowel diseases.

Th17 cell differentiation | gene transcription | Brd4 | bromodomain | chemical inhibitor

CD4$^+$ T cells are important immune cells in biology and have been implicated in the pathology of autoimmune diseases and cancer (1–5). They develop in thymus to different T-helper (Th) cells to guide immune effector functions (6). The known Th effector subsets including Th1, Th2, Th17, and Treg produce signature genes and perform different immune functions (7, 8). Particularly, Th17 cells produce IL-17a and IL-17f and protect mucosa from bacterial and fungal infection (9, 10). Th17 cell development is linked to inflammatory disorders including multiple sclerosis, rheumatoid arthritis, and inflammatory bowel disease (11–13).

Lineage-specific differentiation of naïve CD4$^+$ T cells to Th17 cells is tightly controlled by gene transcription in chromatin (14–16)—a complex process that involves collective activities of key transcription factors Stat3, Batf, and Irf4, as well as Th17-specific orphan nuclear receptor RORγT (17–20). These transcription factors work with chromatin modifying enzymes and effector proteins to ensure proper timing, duration, and amplitude for ordered gene transcription in Th17 cell differentiation (15, 21). Of these are a family of bromodomain (BrD) and extraterminal domain (BET) proteins consisting of Brd2, Brd3, Brd4, and testis-specific Brdt (22, 23). BET proteins play a multifaceted role in gene transcription through their tandem bromodomains binding to lysine-acetylated histones and transcription factors during chromatin opening, transcription factor recruitment to target gene promoter and enhancer sites, and activation of paused RNA polymerase II (PolII) transcriptional machinery for productive gene activation (24, 25). Consistent with their role in T-helper-cell differentiation (26), inhibition of acetyl-lysine binding of the BET proteins by pan-BET BrD inhibitors, such as JQ1, affects differentiation of not only Th17 but also of Th1 and Th2 cells (27, 28). Because of such broad activities, unfortunately, pan-BET BrD inhibitors are thought to have limited therapeutic potential. Whether these BET proteins represent viable new epigenetic drug targets for inflammatory disorders has remained an unanswered question to this day.

Growing evidence shows that the two BrDs of BET proteins have distinct functions in gene transcription in that the second BrD (BD2) of Brd4 is dedicated to interaction with lysine-acetylated transcription factors and p-TEFb, whereas the first BrD (BD1) functions to anchor the activated Brd4/transcription protein

Significance

The bromodomain and extraterminal domain (BET) proteins regulate transcription of subset-specifying genes during lineage-specific T-helper-cell differentiation in adaptor immunity and are also implicated in inflammatory disorders. The available pan-BET bromodomain inhibitors such as JQ1 indiscriminately block the tandem bromodomains (BD1 and BD2) of the BET proteins, broadly render differentiation of different Th subsets, and have limited therapeutic potential. Here we report a small molecule, MS402, that can selectively inhibit BD1 over BD2 of the BET proteins and block Th17 maturation from mouse naive CD4$^+$ T cells, with limited or no effects on Th1, Th2, or Treg cells. MS402 effectively prevents and ameliorates T-cell transfer-induced colitis in mice by disrupting Th17 cell development, thus representing a therapeutic approach for inflammatory bowel diseases.

Author contributions: K.C., H.X., and M.-M.Z. designed research; K.C., G.L., R.S., A.V., R.Z., A.N.P., F.Z., Q.Z., Y.J., Y.H., L. Zhao, X.H., J.M., F.X., A.J., T.S., H.Z., E.R., L. Zeng, J.Z., J.Y., and L.P. performed research; D.Y.Z. contributed new reagents/analytic tools; K.C., G.L., R.S., A.V., R.Z., A.N.P., F.Z., Q.Z., Y.J., Y.H., L. Zhao, X.H., J.M., A.J., T.S., H.Z., E.R., L. Zeng, J.Z., J.Y., L.P., M.O., M.J.W., H.X., and M.-M.Z. analyzed data; and K.C., H.X., and M.-M.Z. wrote the paper.

The authors declare no conflict of interest.

This article is a PNAS Direct Submission.

Data deposition: Crystallography, atomic coordinates, and structure factors have been deposited in the Protein Data Bank, www.pdb.org (PDB ID code 5ULA). The ChIP-seq and RNA-seq data have been deposited in the Gene Expression Omnibus (GEO) database, www.ncbi.nlm.nih.gov/geo (accession nos. GSE90788 and GSE95052, respectively).

[1]K.C. and G.L. contributed equally to this work.

[2]To whom correspondence may be addressed. Email: huabao.xiong@mssm.edu or ming-ming.zhou@mssm.edu.

This article contains supporting information online at www.pnas.org/lookup/suppl/doi:10.1073/pnas.1615601114/-/DCSupplemental.

complex to target genes in chromatin through binding to lysine-acetylated histone H4 (26, 29). We sought to investigate how selective BET BrD inhibition modulates gene transcription in lineage-specific differentiation of different Th subsets. In this study, we have developed a BD1-selective BET BrD inhibitor, MS402, and showed that it can selectively render differentiation of Th17 cells over other Th cells from murine primary naïve $CD4^+$ T cells. We further demonstrated the therapeutic potential of MS402 in preventing and ameliorating adaptive T-cell transfer-induced colitis in mice through the disruption of Brd4 functions in gene transcription and Th17 cell development.

Results and Discussion

Given that the BD1 of the BET proteins is dedicated for binding to lysine-acetylated histone H4 for gene transcriptional activation (30), we reasoned that a small molecule that selectively targets the BD1 could effectively block BET functions in gene activation in chromatin. Using structure-guided design, we developed a cyclopentanone-based BrD inhibitor, MS402 (see its synthesis in Scheme S1), that displays nanomolar inhibitory activity against the BD1 (K_i of 77 nM) with a ninefold selectivity over BD2 of BRD4 (Fig. 1*A*). This selectivity is consistently seen with the BrDs of BRD2 or BRD3, albeit to a lesser extent (Fig. S1*A*). The BrD of CREB-binding protein (CBP) binds MS402 with K_i of 775 nM, 10-fold weaker than BRD4-BD1, and other representative BrDs from different subgroups of the BrD family including PCAF, SMARCA4, BPTF, and BAZ2B show very weak binding to MS402 with 50-fold or more less affinity than BRD4-BD1 (Fig. S1 *A* and *B*). MS402 is 200–300 times more potent than K5ac/K8ac-di-acetylated H4 peptide in binding to BRD4 BrDs (Fig. 1*A*).

Our 1.5-Å-resolution crystal structure of the BRD4 BD1 revealed that MS402 is bound across the ZA channel, establishing interactions with Val87, Leu92, and Leu94 on one side and Trp81, Pro82, Phe83, and Ile146 on the other (Fig. 1*B* and Table S1). The carbonyl oxygen of its cyclopentanone moiety forms two key hydrogen bonds, one with the side-chain amide of the conserved Asn140 and the other mediated by a bound water molecule to the phenoxyl group of Tyr97. In addition, this moiety makes van der Waals contacts with a gatekeeper residue Ile146. The amino group connecting cyclopentanone and chlorobenzene forms another hydrogen bond to the backbone carbonyl oxygen of Pro82 of the WPF shelf. Further, the amide nitrogen linking the two aromatic rings of MS402 forms a water-mediated hydrogen bond to the side-chain carbonyl oxygen of Gln85. The latter is unique in the BD1, corresponding to a Lys in the BD2 that is not engaged in hydrogen bond binding to MS402 as does Gln85 in BD1; point mutation of Gln85 to a Lys or Ala nearly abolished the preferred MS402 binding by BD1 over BD2 (Fig. S1 *B–D*). Further, change of Ile146 in BD1 to smaller Val439 in BD2 likely weakens van der Waals contacts between the protein and cyclopentanone, thus explaining MS402 selectivity for the BD1 over BD2 of BRD4.

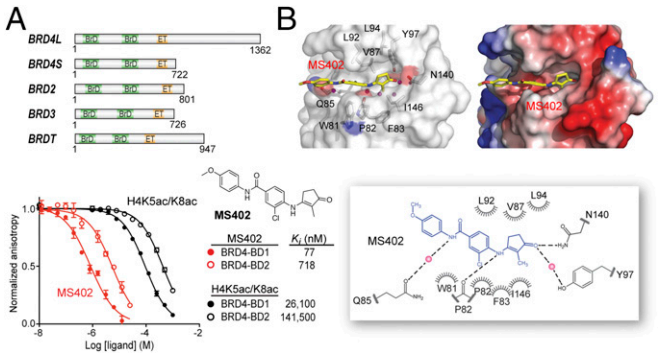

Fig. 1. Structure-guided development of MS402, a BD1-selective BET BrD inhibitor. (*A*) (*Upper*) Domain organization of mammalian BET family proteins. (*Lower*) Binding affinity of MS402 or an H4K5ac/K8ac peptide (residues 1–13) to the BrDs of BRD4 as measured in a fluorescence anisotropy binding assay using an FITC-labeled BrD inhibitor as a probe. (*B*) (*Left*) The crystal structure of MS402 (yellow) bound to the BRD4-BD1. (*Right*) Electrostatic potential surface representation of the BRD4-BD1/MS402 complex. Side chains of key residues at the ligand-binding site in the protein are shown, and bound water molecules are depicted as red spheres. (*Lower*) Schematic diagram highlights key interactions in MS402 recognition by the BRD4-BD1. Two key water molecules are shown in magenta spheres, and hydrogen bonds are drawn as dashed lines. The figure was generated using LIGPLOT (43).

To study the role of BET proteins in Th cell differentiation we isolated murine primary naïve $CD4^+$ T cells from mouse spleen and lymph nodes and treated them with IL-12, IL-4 plus α-IL-12, TGF-β plus IL-6, or TGF-β plus IL-2, respectively, to promote Th1, Th2, Th17, or Treg linage-specific differentiation over 3.5 d with or without MS402 added daily to cell culture (Fig. 2*A*). Strikingly, as shown by flow cytometry analysis, MS402, in a dose-dependent manner, inhibited IL-17 release from 18.6 to 8.0% in the Th17 polarizing condition and to a lesser extent IFN-γ production from 49.7 to 38.6% in the Th1 condition; it had little, if any, effect on IL-4 and Foxp3 expression during Th2 and Treg cell differentiation, respectively (Fig. 2*B*). MS402 did not affect T-cell proliferation as assessed in a carboxy-fluorescein succinimidyl ester dilution assay (Fig. S2*A*).

Notably, MS417, a potent pan-BET BrD inhibitor (K_i <10 nM) (26), and JQ1 (31) and I-BET762 (32) that share the diazepine scaffold, block broadly differentiation of murine primary naïve $CD4^+$ T cells to Th17, Th1, Th2, and, to a lesser extent, Treg cells under the conditions similar to those used for MS402 (Fig. 2*B* and Fig. S2 *B–D*). Our data agree with a report of suppression of Th17-mediated pathology by JQ1 (28). Further, a potent, selective CBP BrD inhibitor, CBP30 (K_d = 26 nM), was reported to suppress Th17 cell differentiation (33). Using the same condition, however, we found that CBP30 inhibits Th17 and also Th2 cell differentiation and has limited effects on Th1 or Treg cells (Fig. S2*E*). These results argue that MS402's modest activity on CBP BrD (K_i of 775 nM, 10-fold weaker than Brd4-BD1) likely does not contribute to its selective activity on Th17 cell differentiation, especially when used at submicromolar concentrations.

The selective activity of MS402 on inhibition of Th17 cell differentiation over Th1, Th2, or Treg cells is further supported by our observations that in a dose-dependent manner MS402 effectively inhibits transcriptional activation of *rorc* and *il17a* in Th17 cells, and to a lesser extent *tbx21* and *ifng* in Th1 cells, and it has only small effects on *gata3* and *il4* expression in Th2 cells, and almost no effects on *foxp3* and *il10* in Treg cells (Fig. 2*C*). These results contrast sharply to the much more broad effects of MS417 on the signature genes of Th17 and Th1 as well as Th2 cells (Fig. 2*C*). We confirmed the inhibitory effects of MS402 on additional key Th17 genes *il17f*, *il21*, *il23r*, *ahr*, *irf4*, and *il9* (Fig. S2*F*). We further observed that MS402 treatment resulted in a marked reduction of Brd4 and Cdk9 occupancy and RNA PolII Ser2 phosphorylation level at the Stat3 binding sites in *il17a/f* and *rorc* loci (Fig. S2*G*), which is required for transcription elongation (26). Notably, MS402 seems to have minimal effects on genomic occupancy of Brd2 (Fig. S2*G*). Further, MS402 inhibition is independent of IL-10 expression and does not involve IL-27 or IL-35, because it is still able to suppress Th17 and Th1 cell differentiation in *il10*$^{-/-}$ mice (Fig. S2*H*) and inhibit activation of *il-17a*, *il17*, *rorc*, *ifng*, and *T-bet* in *EBI3*$^{-/-}$ mice (Fig. S2*I*).

We next performed genomic sequencing analysis to better understand how MS402 and JQ1 affect gene transcription in Th17 cell differentiation. Specifically, we carried out chromatin immunoprecipitation sequencing (ChIP-seq) for Brd4 and RNA-seq experiments for mouse Th17 cells with and without MS402 or JQ1 treatment. Overall, MS402 and JQ1 treatments yielded a similar pattern of perturbation in gene transcription in Th17 cell differentiation (Fig. 3*A* and Fig. S3 *A–D*), albeit certain Th17 signature cytokine genes such as *il17a,f* and *il22* are perturbed slightly even more by MS402 than by JQ1 (Fig. 3*B*). Immune and cytokine ontologies seem consistently more enriched in the set of genes down-regulated by MS402 compared with JQ1 (Fig. 3*C*), whereas genes up-regulated are clustered in cell development and maturation

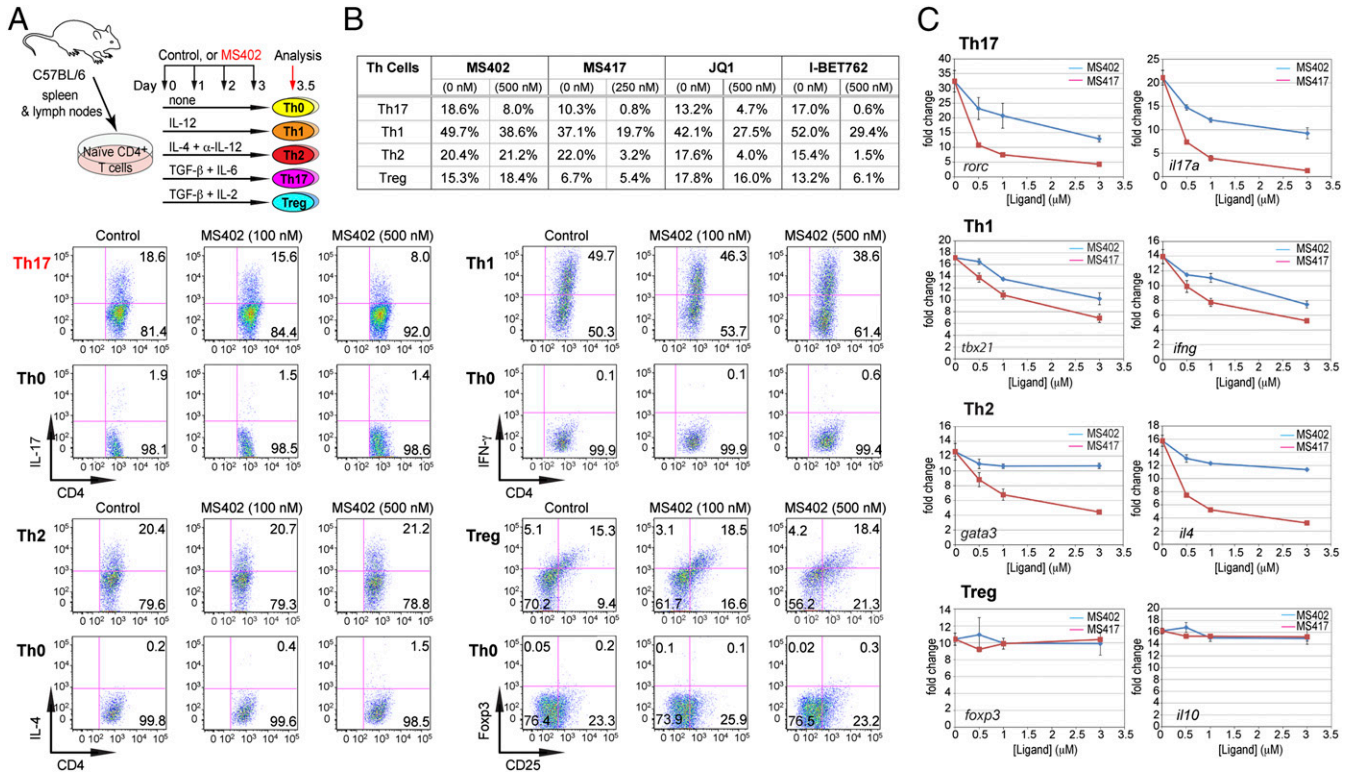

Th Cells	MS402		MS417		JQ1		I-BET762	
	(0 nM)	(500 nM)	(0 nM)	(250 nM)	(0 nM)	(500 nM)	(0 nM)	(500 nM)
Th17	18.6%	8.0%	10.3%	0.8%	13.2%	4.7%	17.0%	0.6%
Th1	49.7%	38.6%	37.1%	19.7%	42.1%	27.5%	52.0%	29.4%
Th2	20.4%	21.2%	22.0%	3.2%	17.6%	4.0%	15.4%	1.5%
Treg	15.3%	18.4%	6.7%	5.4%	17.8%	16.0%	13.2%	6.1%

Fig. 2. MS402, a bromodomain inhibitor, renders Th17 cell differentiation. (*A*) (*Upper*) A schematic illustration of the T-helper-cell differentiation study. (*Lower*) Flow cytometry analysis of mouse primary naïve $CD4^+$ T cells purified from spleens and lymph nodes of C57BL/6 mice and differentiated under Th0, Th1, Th2, Th17, and Treg polarization conditions with and without the presence of MS402 added daily at 100 nM or 500 nM. (*B*) Table summarizing the effects of MS402 or pan-BET BrD inhibitors including MS417, JQ1, and I-BET762 on T-helper-cell differentiation. (*C*) Effects of MS402 or MS417 treatment on mRNA expression levels of key Th17, Th1, Th2, or Treg subset-specific signature genes (transcription factors and cytokines) after 3-d lineage-specific cell differentiation from mouse primary naïve $CD4^+$ T cells in a dose-dependent manner.

(Fig. S3*E*). Further, Venn diagram analyses reveal that a majority of MS402-altered genes, with up or down transcriptional expression upon compound treatment, are covered by JQ1, but almost half of JQ1-affected genes are unchanged by MS402 (Fig. 3*D*). Notably, violin plot analysis of the RNA-seq data and comparison of the ChIP-seq data show that MS402 is effective similarly to JQ1 in releasing Brd4 genomic occupancy at Th17 signature genes and super enhancers but has fewer effects than JQ1 at housekeeping genes (Fig. 3*E* and Fig. S3 *F–H*). This apparently selective effect of MS402 over JQ1 is illustrated by representative RNA-seq tracks showing Th17 signature genes *Batf* and *Rorc* whose transcription is effectively down-regulated by MS402 or JQ1, whereas a housekeeping gene *Oxsm* is down-regulated by JQ1 but much less by MS402 (Fig. 3*F*). Given that MS402 exhibited cellular inhibitory effects on the order of its affinity for the BD1 of BET proteins, our results collectively suggest that pharmacological inhibition of the BD1 of BET proteins by MS402, likely blocking Brd4 activity required for Th17 signature gene transcriptional activation, is sufficient to render Th17 cell differentiation.

We next examined in vivo effects of MS402 in a T-cell transfer-induced colitis model in mice (Fig. 4*A*), in which Th17 cells are implicated in disease progression (11–13). After reconstitution with naïve $CD4^+CD45RB^{hi}$ cells isolated from spleen and lymph nodes of C57BL/6 mice, *Rag1*$^{-/-}$ mice began losing weight after 4 wk, whereas the mice that received MS402 intraperitoneally twice a week at 10 mg/kg showed much less weight loss (Fig. 4*B*). Histology analysis revealed that 7 wk after reconstitution the colon of the T-cell transfer group mice was markedly shorter and inflamed compared with the control, whereas the colons of MS402-treated mice showed little difference in length or appearance (Fig. 4*C*). Notably, unlike the disease mice that exhibited severe inflammation at the end of the study with a disease score of 3, the MS402-treated mice displayed only mild or almost negative inflammation with a disease score of 0–1 (Fig. 4*D*). Histological study of colon sections from the disease mice confirmed more severe inflammatory cell infiltrates and significantly higher pathological scores than colons of those treated with MS402 (Fig. 4*E*). Finally, the MS402-treated mice showed a significantly lower percentage of IL-17- and IFN-γ–producing $CD4^+$ T cells in colon than the disease mice (Fig. 4*F*). Taken together, these results showed that MS402 is effective in vivo, blocking Th17 cell development required for T-cell transfer-induced colitis in mice.

We conducted another in vivo experimental colitis study to explore therapeutic potential of MS402. In this study we started MS402 treatment at week 5 when the *Rag1*$^{-/-}$ mice had developed colitis, as judged by marked weight loss, with i.p. injections twice a week at 10 mg/kg for 3 wk (Fig. 4*A*). Notably, the mice treated with MS402 exhibited a reversal of weight loss after 1 wk (Fig. 4*G*). Consistently, the MS402-treated mice showed an almost minimal degree of inflammation in the colon, as demonstrated by much improved colon length and appearance (Fig. S4*A*), a lower disease score of 0–1 (Fig. S4*B*), and markedly reduced inflammatory cell infiltrates in colon sections as compared with those of the disease-group mice (Fig. 4*H*). Further, the MS402-treated mice also had a lower population of IFN-γ–producing $CD4^+$ T cells and exhibited a much more dramatic reduction of IL-17–producing $CD4^+$ T cells in colon than the group of T-cell-transfer disease mice (Fig. 4*I*). It is worth noting that the selectivity of MS402 for Th17 over Th1 cells is more profound in this therapeutic treatment model than that in the preventive model (Fig. 4*I* vs. Fig. 4*F*). This differential effect seems to be consistent with the selectivity of MS402 on the maintenance of Th17 over Th1 cells compared with broad effects by pan-BET inhibitor JQ1 after these Th cells are differentiated ex vivo from the mouse primary naïve $CD4^+$ T cells (Fig. S4*C*). Finally, the

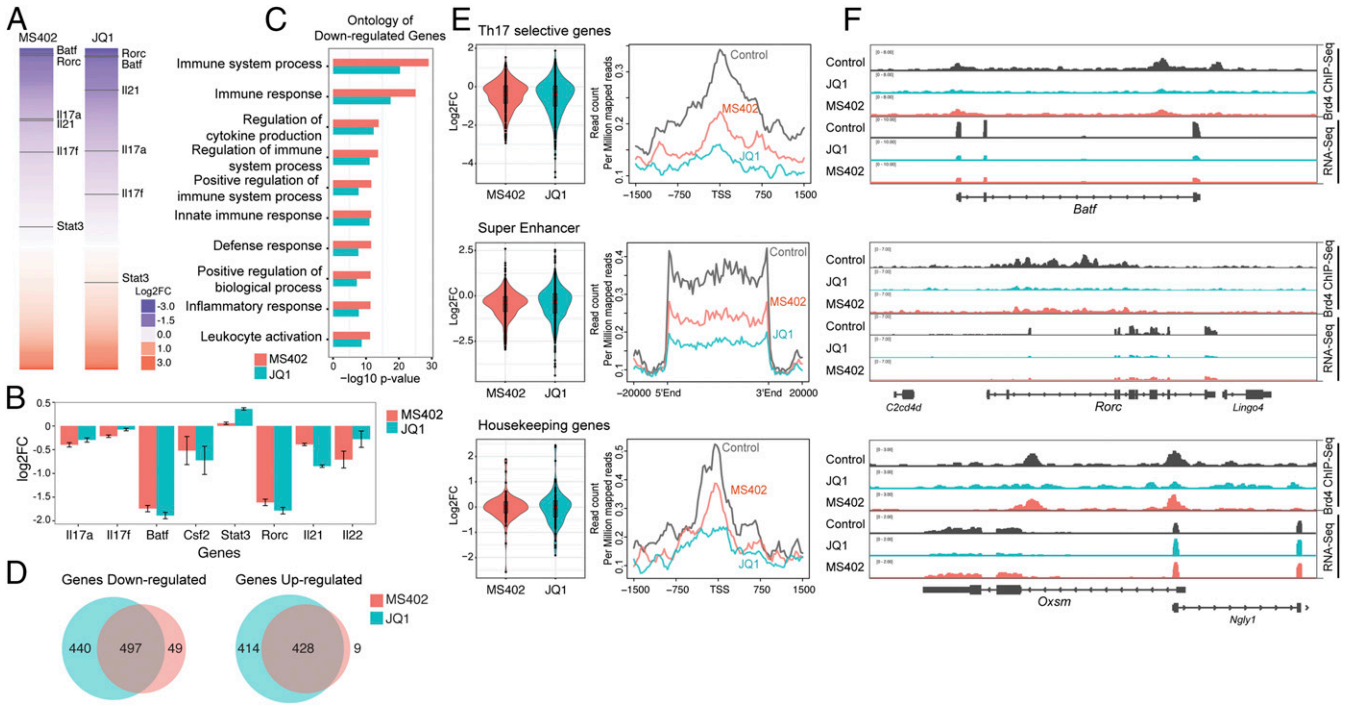

Fig. 3. Genomic analysis of BET inhibition effects on gene transcription during Th17 cell differentiation. (*A*) Effects of MS402 and JQ1 treatment on gene transcription in Th17 cell differentiation. Genes are ranked from most down-regulated to most up-regulated by compound treatment. Select Th17 signature genes whose transcriptional levels are affected by compound treatment are indicated. (*B*) MS402 and JQ1 show comparable (log2) fold change for select Th17 signature genes. (*C*) Immune and cytokine ontologies are among top-enriched down-regulated genes by MS402 or JQ1 treatment. (*D*) Venn diagram analysis of genes down- or up-regulated by MS402 and JQ1 treatment during Th17 differentiation. (*E*) Violin plots of the RNA-seq data and profiles of the ChIP-seq data showing patterns of perturbation across multiple gene sets of Th17 selective genes, genes with super enhancers, and housekeeping genes in Th17 cells upon treatment of MS402 or JQ1. (*F*) Select RNA-seq tracks illustrating changes of transcriptional expression of Brd4 target genes *Batf* and *Rorc* (Th17 selective genes) and Oxsm (housekeeping) upon the treatment of MS402 or JQ1.

MS402-treated mice had much lower mRNA expression levels of key cytokines and Th17- and Th1-specific transcription factors including *il17*, *il21*, *il22*, *il6*, *rorc*, *Tbet*, and *ifng* compared with the disease-group mice (Fig. 4*J*). Collectively, these results show that MS402 is an effective inhibitor of Th17 cell development and ameliorates adaptive T-cell transfer-induced colitis in mice.

Notably, it was recently reported that BET inhibition by JQ1 caused an increased progression of dextran sodium sulfate (DSS)-induced colitis in mice (34). Although the acute DSS colitis model is useful for study of the innate immune system in the development of intestinal inflammation, T and B cells are not required for the colitis development in this model (35). Nevertheless, these results highlight multifaceted functions of the BET proteins in adaptive and innate immunity and inflammatory pathology. Further investigation is warranted to determine the mechanistic details of the BET proteins in different functional contexts.

In summary, in this study we show that the BrDs of the BET proteins likely have distinct functions in gene transcription during differentiation of naïve $CD4^+$ T cells to different T-helper cells, and that the BD1 of Brd4 is central to Th17 cell differentiation and both BD1 and BD2 are important for Th1 and Th2 cell differentiation, whereas neither is essential for Treg cell differentiation. Notably, the BET proteins likely function differently in Th17 cells. Unlike Brd4, Brd2 genomic occupancy is minimally affected by BET inhibition, whereas as reported Brd3 has little expression in Th17 cells (28). Accordingly, our newly designed BD1-specific inhibitor MS402 is effective and sufficient to render Th17 cell differentiation likely through blocking Brd4 binding to Th17 signature gene loci whose transcriptional activation is required for Th17 cell differentiation. We further showed that selective chemical inhibition of the BD1 of Brd4 by MS402 can effectively prevent and ameliorate T-cell transfer-induced colitis in mice by blocking Th17, and to lesser extent Th1 cell development. Collectively, our study suggests a therapeutic strategy of selective targeting the BD1 of the BET proteins as a promising targeted therapy for inflammatory bowel diseases including colitis that lack a safe and effective treatment.

Materials and Methods

Methods and associated references are available in *SI Materials and Methods*.

Mice. C57BL/6 wild-type, *il10*$^{-/-}$, and *EBI3*$^{-/-}$ mice were obtained from Jackson Laboratory.

Compound. The chemical synthesis and characterization of MS402 is provided in Scheme S1 and Fig. S5.

Cell Sorting and T-Helper-Cell Differentiation. $CD4^+$ T cells were purified from mouse spleen and lymph nodes using anti-CD4 microbeads (Miltenyi Biotech). Naïve $CD4^+$ T cells were activated with plate-bound anti-CD3 (1.5 μM/mL) and anti-CD28 (1.5 μM/mL) plus cytokines IL-12 (20 ng/mL) and anti-IL4 (10 μM/mL) for Th1 conditions, IL4 (20 ng/mL), anti-IL12 (10 μM/mL), and anti–IFN-γ (10 μM/mL) for Th2 conditions, IL6 (20 ng/mL) and TGF-β (2.5 ng/mL) for Th17 conditions, and TGF-β (2.5 ng/mL) for Treg conditions. The cells were cultured for 2–3 d before harvesting for analysis. All cytokines were purchased from R&D, and neutralizing antibodies were purchased from BD Pharmigen.

Intracellular Staining and Flow Cytometry. Cells were stimulated with phorbol myristate acetate (PMA) and ionomycin for 5 h in the presence of brefeldin A before intracellular staining. Cells were fixed with IC Fixation Buffer (BD Biosciences), incubated with permeabilization buffer, and stained with PE-anti-mouse IL-17, APC-anti-IFN-γ, and PE-Cy 5.5 anti-mouse CD4 antibodies. Flow cytometry was performed on a FACSCalibur and BD LSR Fortessa (BD Biosciences).

Real-Time Quantitative PCR (qPCR). Total RNA was extracted with RNeasy Mini Kit (Qiagen) and reverse-transcribed using the SuperScript III Reverse Transcriptase (Life Technologies). All qPCR analyses were performed using Brilliant III Ultra Fast SYBR Green QPCR Master Mix (Agilent Technologies). In gene

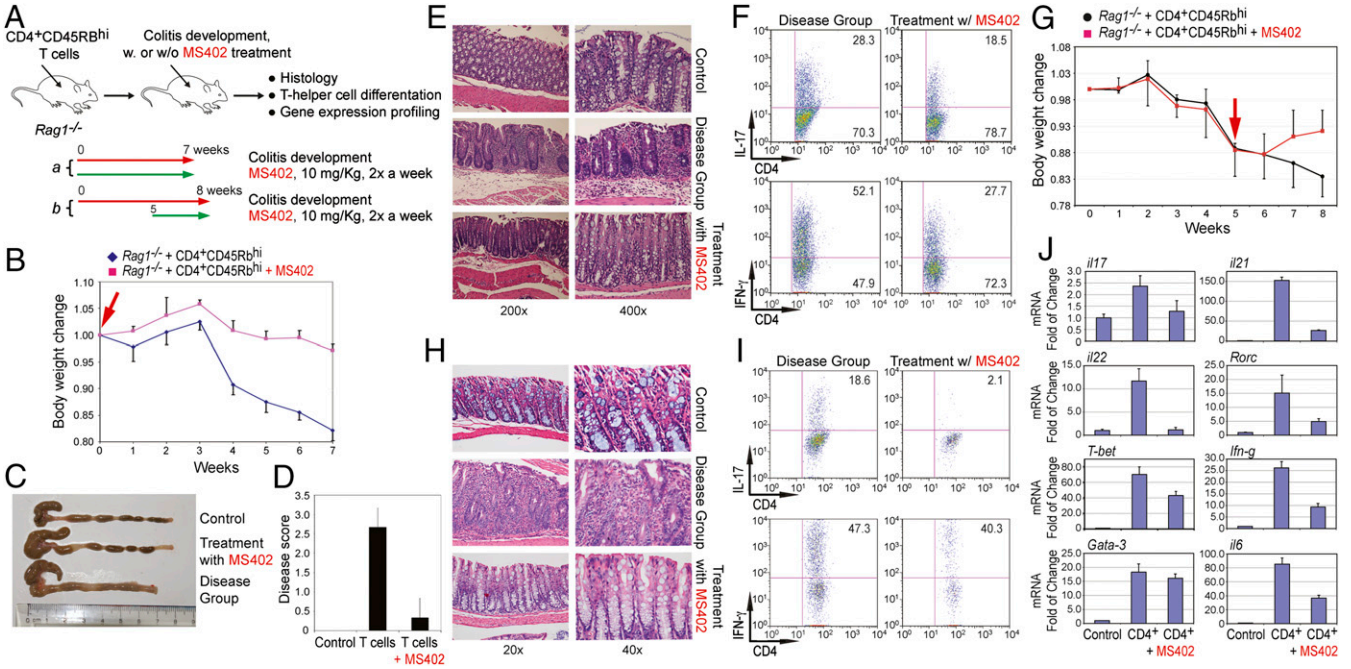

Fig. 4. MS402 ameliorates adaptive T-cell transfer-induced colitis in mice. (*A*) Scheme illustrating the experimental colitis study. $CD4^+CD45RB^{hi}$ T cells were purified from spleens and lymph nodes of wild-type or *iNOS*$^{-/-}$ mice and 5×10^5 cells were injected (i.p.) into recipient *Rag1*$^{-/-}$ mice. Mice were treated with PBS in a control group or MS402 (10 mg/kg) twice a week starting either at week 0 (*a*), or week 5 (*b*) for 7 or 3 wk, respectively. Body weight change was monitored weekly, and mice were killed at the end of experiment for histology analysis. (*B*) Changes in body weight of *Rag1*$^{-/-}$ mice ($n = 5$–6 mice per group) after i.p. transfer of wild-type $CD4^+CD45RB^{hi}$ T cells were recorded. MS402 treatment started at week 0 for 7 wk. Data are presented as the mean ± SD of the percentage of initial body weight and are representative of two similar experiments. (*C*) Changes of morphology of intestines of the *Rag1*$^{-/-}$ mice with and without MS402 treatment as in *B*. (*D*) Disease score assessing efficacy of MS402 treatment as in *B* on ameliorating inflammation of colitis in mice. The inflammation grading was graded on a scale of 0–3: negative (0), no inflammation; mild (1), mild and patchy; moderate (2), most crypts involved by inflammation; or severe (3), crypt abscess, ulceration, erosion, or submucosal involvement. The inflammation cells are most lymphocytes with some neutrophils. (*E*) Images showing H&E staining of large intestines of the *Rag1*$^{-/-}$ mice with or without MS402 treatment as in *B*. (*F*) Flow cytometry analysis of $CD4^+IL17^+$ and $CD4^+IFN\gamma^+$ T cells in large intestine from the *Rag1*$^{-/-}$ mice treated with or without MS402 treatment as in *B*. All results are statistically significant ($P < 0.05$) and are representative of more than two independent experiments. (*G*) Body weight change over time after $CD4^+$ T cells injected into recipient *Rag1*$^{-/-}$ mice with and without MS402 treatment, as indicated by a red arrow (i.e., started at week 5 until week 8). (*H*) Images showing H&E staining of large intestines of the *Rag1*$^{-/-}$ mice with or without MS402 treatment as in *G*. (*I*) Flow cytometry analysis of $CD4^+IL17^+$ and $CD4^+IFN\gamma^+$ T cells in large intestine from the *Rag1*$^{-/-}$ mice treated with or without MS402 starting at week 5 as in *G*. All results are statistically significant ($P < 0.05$) and are representative of more than two independent experiments. (*J*) mRNA levels of Th17 and Th1-specific genes measured in the *Rag1*$^{-/-}$ mice treated with or without MS402 starting at week 5 as in *G*.

expression analysis all data were normalized with Actin/Gapdh and represented relative to the control sample (fold change). For ChIP-qPCR relative occupancies were calculated as ratio of the amount of immunopreciptated DNA to that of the input sample (percent input). Measurements were performed in duplicate, and error bars denote experimental SDs. Results are representative of more than two independent experiments. Primer sequences are available in Table S2.

ELISA. All ELISA kits were purchased from eBioscience and experiments were performed according to protocols provided by the manufacturer. Briefly, supernatants of samples were incubated in plates coated with capture antibody. Detection antibody was added after a total of five washes. Avidin-HRP was then added after a total of five washes. Plates were read at 450 nm after addition of substrate solution and stop solution. Concentration of the cytokines in samples was calculated with reference to the absorbance value obtained from the standard curve.

ChIP. Cells were chemically cross-linked with 1% formaldehyde solution for 10 min at room temperature followed by the addition of 2.5 M glycine (to a final concentration of 125 mM) for 5 min. Cells were rinsed twice with cold 1× PBS and then lysed in Szak's RIPA buffer [150 mM NaCl, 1% Nonidet P-40, 0.5% deoxycholate, 0.1% SDS, 50 mM Tris·HCl, pH 8, 5 mM EDTA, Protease Inhibitor mixture (Roche), and 10 mM PMSF]. Cells were then sonicated using sonicator (QSonica) for 10 pulses of 15 s at a voltage of 70 V, followed by a 1-min rest on ice. Sonicated chromatin was cleared by centrifugation. The resulting chromatin extract was incubated overnight at 4 °C with appropriate primary antibody (anti-Brd4 or IHC-00396) and 25 μL of Protein G and 25 μL of Protein A magnetic beads (Dynabeads; Life Technologies). Beads were washed two times with incomplete Szak's RIPA buffer (without PMSF and Protease Inhibitor mixture), four times with Szak's IP Wash Buffer (100 mM Tris·HCl, pH 8.5, 500 mM LiCl, 1% Nonidet P-40, and 1% deoxycholate), then twice again with incomplete RIPA buffer and twice with cold 1× Tris-EDTA. Complexes were eluted from beads in Talianidis Elution Buffer by heating at 65 °C for 10 min and then by adding NaCl to a final concentration of 200 mM and reverse cross-linking was performed overnight at 65 °C. Input DNA was concurrently treated for cross-link reversal. Samples were then treated with RNaseA and proteinase K for an hour, extracted with phenol/chloroform, and ethanol-precipitated. The pellet was resuspended in water and used for subsequent ChIP-seq library preparation or analyzed by qPCR as described above.

T-Cell-Transfer Colitis Studies and Histopathology. T-cell-transfer colitis was performed as previously described (36, 37). Briefly, purified $CD4^+CD45RB^{hi}$ T cells from C57/B6 mice were injected i.p. into *Rag1*$^{-/-}$ recipients (5×10^5 cells per mouse in 200 μL sterile PBS per injection). Mice were weighed every week throughout the course of experiments. After 5–7 wk, mice were killed and colon tissues were excised. Tissues were fixed in 10% (vol/vol) buffered formalin and paraffin-embedded. The sections (5 μm) of tissue samples were stained with H&E. All of the slides were read and scored by an experienced pathologist without previous knowledge of the type of treatment. The degree of inflammation in the epithelium, submucosa, and muscularis propria was scored separately.

Sequencing Library Preparation and Sequencing. ChIPed-DNA was end-repaired with T4 DNA polymerase and polynucleotide kinase. An A-base was added to the end-repaired DNA fragments. Solexa adaptors were ligated to the DNA fragments and 200- to 300-bp size fractions were obtained using E-gel (Life Technologies). Adaptor-modified fragments were enriched by 18 cycles of PCR amplification. The DNA library prep was validated in Bioanalyzer for quantity and size. The input- and ChIPed-DNA libraries were sequenced on the Illumina

HiSeq2000 platform with 50-bp read length in a single end mode. RNA-seq libraries were prepared from TRIzol-extracted RNA samples from which rRNA was removed using Ribo-ZeroTM and following the TruSeq Stranded Total RNA Sample Prep kit protocol (Illumina). The input- and ChIP-DNA libraries were sequenced on the Illumina HiSEq. 2000 platform with 50-bp read length in a single end mode. Sequencing of RNA libraries was performed on the Illumina HiSEq. 2000 platform with 100-bp read length in a paired end mode. All ChIP-seq and RNA-seq data in this study are deposited in the Gene Expression Omnibus under the accession nos. GSE90788 and GSE95052, respectively.

Bioinformatics Analysis. For ChIP-seq analysis the input and ChIP samples were sequenced by Illumina HiSeq200. After QC filtering by FASTAX (hannonlab.cshl.edu/fastx_toolkit/), only the reads with a quality score Q20 in at least 90% bases were included for analysis. The reads from both input and ChIP samples were filtered and trimmed using Trimmomatic (38) and then aligned to mm9 reference genome using Bowtie. The peaks in the ChIP sample in reference to the input sample were called from read alignments by MACS algorithm (v1.4) and then the distance to the closest transcription start site (TSS) was annotated from genome mapping information of RefSeq transcripts. Genes associated with peaks were annotated (amp.pharm.mssm.edu/Enrichr/). Peaks were chosen with the criteria false discovery rate (FDR) <0.01 and *P* value <0.005. ChIP-seq from published work was taken from GSE60482 (Th17 p300) (15, 39). This was treated the same as in-house-generated ChIP-Seq. Finally, the alignment and coverage of ChIPseq data were visualized by Integrative Genomics Viewer (software.broadinstitute.org/software/igv/). Gene annotation and pathway analysis of the identified genes was performed using the Database for Annotation, Visualization and Integrated Discovery (https://david.ncifcrf.gov/). For RNA-Seq analysis the reads were filtered and trimmed using Trimmomatic (38) and aligned to the mm9 mouse reference genome and indexes based on UCSC annotations using TopHat (40). HTSeq (41) was used to find the read counts across the UCSC reference genome. Differentially expressed genes were identified by the R package DESeq2 (42) using an FDR <0.1 and fold change >1.5. RNA-Seq from Th1 and Th2 cells was taken from GSE40463. These data were analyzed in the same way as in-house-generated data. Heat maps were derived by sorting all genes with counts ≥5 by log-fold change for each compound treatment.

Statistical Analysis. Statistical analysis was performed using Student's *t* test. *P* values <0.05 were considered statistically significant.

Data Deposition. Structure factors and coordinates for the BRD4-BD1/MS402 complex have been deposited in the Protein Data Bank (PDB ID code 5ULA).

Study Approval. Mouse experiments were approved by the Institutional Animal Care and Use Committees of the Icahn School of Medicine at Mount Sinai.

ACKNOWLEDGMENTS. We thank Dr. J. Jakoncic and the staff at the X6A beamline of the National Synchrotron Light Sources at the Brookhaven National Laboratory for assisting with X-ray data collection. This work was supported in part by the research fund from the First Hospital of Jilin University, and the research grants from the National Natural Science Foundation of China (81601409) (to L. Zhao) and the US National Institutes of Health (to L. Zeng, M.J.W., H.X., and M.-M.Z.).

1. Iwasaki A, Medzhitov R (2015) Control of adaptive immunity by the innate immune system. *Nat Immunol* 16(4):343–353.
2. Tabas I, Glass CK (2013) Anti-inflammatory therapy in chronic disease: Challenges and opportunities. *Science* 339(6116):166–172.
3. Abraham C, Medzhitov R (2011) Interactions between the host innate immune system and microbes in inflammatory bowel disease. *Gastroenterology* 140(6):1729–1737.
4. Rubin DC, Shaker A, Levin MS (2012) Chronic intestinal inflammation: Inflammatory bowel disease and colitis-associated colon cancer. *Front Immunol* 3:107.
5. Saleh M, Trinchieri G (2011) Innate immune mechanisms of colitis and colitis-associated colorectal cancer. *Nat Rev Immunol* 11(1):9–20.
6. Takahama Y (2006) Journey through the thymus: Stromal guides for T-cell development and selection. *Nat Rev Immunol* 6(2):127–135.
7. Park H, et al. (2005) A distinct lineage of CD4 T cells regulates tissue inflammation by producing interleukin 17. *Nat Immunol* 6(11):1133–1141.
8. Harrington LE, et al. (2005) Interleukin 17-producing CD4+ effector T cells develop via a lineage distinct from the T helper type 1 and 2 lineages. *Nat Immunol* 6(11):1123–1132.
9. Murphy KM, Reiner SL (2002) The lineage decisions of helper T cells. *Nat Rev Immunol* 2(12):933–944.
10. Wilson CB, Rowell E, Sekimata M (2009) Epigenetic control of T-helper-cell differentiation. *Nat Rev Immunol* 9(2):91–105.
11. Miossec P, Kolls JK (2012) Targeting IL-17 and TH17 cells in chronic inflammation. *Nat Rev Drug Discov* 11(10):763–776.
12. Dong C (2008) TH17 cells in development: An updated view of their molecular identity and genetic programming. *Nat Rev Immunol* 8(5):337–348.
13. Littman DR, Rudensky AY (2010) Th17 and regulatory T cells in mediating and restraining inflammation. *Cell* 140(6):845–858.
14. Medzhitov R, Horng T (2009) Transcriptional control of the inflammatory response. *Nat Rev Immunol* 9(10):692–703.
15. Ciofani M, et al. (2012) A validated regulatory network for Th17 cell specification. *Cell* 151(2):289–303.
16. Kanno Y, Vahedi G, Hirahara K, Singleton K, O'Shea JJ (2012) Transcriptional and epigenetic control of T helper cell specification: Molecular mechanisms underlying commitment and plasticity. *Annu Rev Immunol* 30:707–731.
17. Yang XO, et al. (2007) STAT3 regulates cytokine-mediated generation of inflammatory helper T cells. *J Biol Chem* 282(13):9358–9363.
18. Schraml BU, et al. (2009) The AP-1 transcription factor Batf controls T(H)17 differentiation. *Nature* 460(7253):405–409.
19. Brüstle A, et al. (2007) The development of inflammatory T(H)-17 cells requires interferon-regulatory factor 4. *Nat Immunol* 8(9):958–966.
20. Okamoto K, et al. (2010) IkappaBzeta regulates T(H)17 development by cooperating with ROR nuclear receptors. *Nature* 464(7293):1381–1385.
21. Yosef N, et al. (2013) Dynamic regulatory network controlling TH17 cell differentiation. *Nature* 496(7446):461–468.
22. Dhalluin C, et al. (1999) Structure and ligand of a histone acetyltransferase bromodomain. *Nature* 399(6735):491–496.
23. Smith SG, Zhou MM (2016) The bromodomain: A new target in emerging epigenetic medicine. *ACS Chem Biol* 11(3):598–608.
24. Hargreaves DC, Horng T, Medzhitov R (2009) Control of inducible gene expression by signal-dependent transcriptional elongation. *Cell* 138(1):129–145.
25. Hnisz D, et al. (2013) Super-enhancers in the control of cell identity and disease. *Cell* 155(4):934–947.
26. Zhang W, et al. (2012) Bromodomain-containing protein 4 (BRD4) regulates RNA polymerase II serine 2 phosphorylation in human CD4+ T cells. *J Biol Chem* 287(51):43137–43155.
27. Bandukwala HS, et al. (2012) Selective inhibition of CD4+ T-cell cytokine production and autoimmunity by BET protein and c-Myc inhibitors. *Proc Natl Acad Sci USA* 109(36):14532–14537.
28. Mele DA, et al. (2013) BET bromodomain inhibition suppresses TH17-mediated pathology. *J Exp Med* 210(11):2181–2190.
29. Schröder S, et al. (2012) Two-pronged binding with bromodomain-containing protein 4 liberates positive transcription elongation factor b from inactive ribonucleoprotein complexes. *J Biol Chem* 287(2):1090–1099.
30. Sanchez R, Zhou MM (2009) The role of human bromodomains in chromatin biology and gene transcription. *Curr Opin Drug Discov Devel* 12(5):659–665.
31. Filippakopoulos P, et al. (2010) Selective inhibition of BET bromodomains. *Nature* 468(7327):1067–1073.
32. Nicodeme E, et al. (2010) Suppression of inflammation by a synthetic histone mimic. *Nature* 468(7327):1119–1123.
33. Hammitzsch A, et al. (2015) CBP30, a selective CBP/p300 bromodomain inhibitor, suppresses human Th17 responses. *Proc Natl Acad Sci USA* 112(34):10768–10773.
34. Wienerroither S, et al. (2014) Regulation of NO synthesis, local inflammation, and innate immunity to pathogens by BET family proteins. *Mol Cell Biol* 34(3):415–427.
35. Chassaing B, Aitken JD, Malleshappa M, Vijay-Kumar M (2014) Dextran sulfate sodium (DSS)-induced colitis in mice. *Curr Protoc Immunol* 104(Unit 15):25.
36. Totsuka T, et al. (2007) IL-7 Is essential for the development and the persistence of chronic colitis. *J Immunol* 178(8):4737–4748.
37. Powrie F, Leach MW, Mauze S, Caddle LB, Coffman RL (1993) Phenotypically distinct subsets of CD4+ T cells induce or protect from chronic intestinal inflammation in C. B-17 scid mice. *Int Immunol* 5(11):1461–1471.
38. Bolger AM, Lohse M, Usadel B (2014) Trimmomatic: A flexible trimmer for Illumina sequence data. *Bioinformatics* 30(15):2114–2120.
39. Wei L, et al. (2010) Discrete roles of STAT4 and STAT6 transcription factors in tuning epigenetic modifications and transcription during T helper cell differentiation. *Immunity* 32(6):840–851.
40. Trapnell C, Pachter L, Salzberg SL (2009) TopHat: Discovering splice junctions with RNA-Seq. *Bioinformatics* 25(9):1105–1111.
41. Anders S, Pyl PT, Huber W (2015) HTSeq–a Python framework to work with high-throughput sequencing data. *Bioinformatics* 31(2):166–169.
42. Love MI, Huber W, Anders S (2014) Moderated estimation of fold change and dispersion for RNA-seq data with DESeq2. *Genome Biol* 15(12):550.
43. Wallace AC, Laskowski RA, Thornton JM (1995) LIGPLOT: A program to generate schematic diagrams of protein-ligand interactions. *Protein Eng* 8(2):127–134.
44. Zeng L, Zhang Q, Gerona-Navarro G, Moshkina N, Zhou MM (2008) Structural basis of site-specific histone recognition by the bromodomains of human coactivators PCAF and CBP/p300. *Structure* 16(4):643–652.
45. Zhang G, et al. (2012) Down-regulation of NF-κB transcriptional activity in HIV-associated kidney disease by BRD4 inhibition. *J Biol Chem* 287(34):28840–28851.
46. Nikolovska-Coleska Z, et al. (2004) Development and optimization of a binding assay for the XIAP BIR3 domain using fluorescence polarization. *Anal Biochem* 332(2):261–273.
47. Huynh K, Partch CL (2015) Analysis of protein stability and ligand interactions by thermal shift assay. *Curr Protoc Protein Sci* 79:28.9.1–14.
48. Otwinowski Z, Minor W (1997) [20] Processing of X-ray diffraction data collected in oscillation mode. *Methods Enzymol* 276:307–326.
49. Vagin A, Teplyakov A (1997) MOLREP: An automated program for molecular replacement. *J Appl Cryst* 30(6):1022–1025.
50. Murshudov GN, Vagin AA, Dodson EJ (1997) Refinement of macromolecular structures by the maximum-likelihood method. *Acta Crystallogr D Biol Crystallogr* 53(Pt 3):240–255.
51. Emsley P, Cowtan K (2004) Coot: Model-building tools for molecular graphics. *Acta Crystallogr D Biol Crystallogr* 60(Pt 12 Pt 1):2126–2132.